

Available online at www.sciencedirect.com

Procedia Computer
Science

Procedia Computer Science 1 (2012) 837–844

www.elsevier.com/locate/procedia

International Conference on Computational Science, ICCS 2010

Unstructured mesh generation from the *Virtual Family* models for whole body biomedical simulations

Dominik Szczerba^{a,b}, Esra Neufeld^a, Marcel Zefferer^a, Gabor Szekely^b, Niels Kuster^a^aIT'IS Research Foundation, Zurich, Switzerland^bComputer Vision Lab, ETH, Zurich, Switzerland

Abstract

Physiological systems are inherently complex, involving multi-physics phenomena at a multitude of spatial and temporal scales. To realistically simulate their functions, detailed high quality multi-resolution often patient specific human models are required. Mesh generation has remained a central topic in finite element analysis (FEA) for a few decades now. Recent developments in high performance computing (HPC) driven by the need for multi-physics multi-scale simulations of physiological systems define new challenges in this area. Even though many algorithms have been developed over years and are offered as commercial packages, they are often limited to mechanical engineering applications only. Mesh generation for human anatomical domains requires more effective and flexible techniques to tackle their greater geometrical and topological complexities. We present, evaluate and discuss several methods to generate unstructured body fitted multi-domain adaptive meshes with geometrically and topologically compatible interfaces from the segmented cross-sections of the *Virtual Family* models for the purpose of large scale whole body simulations. We found that an automated solution is difficult to achieve with real-image qualities, but if optimal methods are selected, good results can be achieved with minimal user-interactions. Therefore we believe that our observations can serve as guidance when choosing an optimal method for a specific application.

© 2012 Published by Elsevier Ltd. Open access under [CC BY-NC-ND license](#).

Keywords: biomedical simulation, whole body anatomical model, unstructured mesh generation, FEA, FEM, compatible triangulation, multi-label medical image data, multi-physics multi-scale simulation.

1. Introduction

Physiological systems are inherently complex. To realistically simulate their functions, detailed high quality human models (preferably patient specific) are required. The freely available Virtual Family Models are based on complete magnetic resonance (MR) datasets of human volunteers representing different sexes, ages, weights, body fat content and developmental stages [1]. Additional models are continuously being added, including more child models of different ages (*Virtual Classroom*), pregnant women models with fetuses at different gestational stages, an obese model and several animal models. All the models originate from high resolution magnetic resonance imaging (MRI) scans (0.5 – 0.9 mm pixel size, 1 – 2 mm slice thickness) of healthy volunteers. They have been acquired in separate blocks (head, extremities...) of varying quality, resolution and sometimes orientation. Overall, the images have a rather low signal to noise ratio and additionally are sometimes blurred. The resolution was not always sufficient to identify fine structures and small features. Especially, vessels and nerves were very difficult to follow continuously. Segmentation errors are estimated to be in order of 1 – 5 mm. It should be stressed, however, that some of the accuracy

loss was not related to the actual imaging modality as such but to the use of conscious volunteers which implied limitations on the scanning time, necessary repositioning, breathing movements, no use of bowel movement reducing agents in the children etc. The anatomical sites in the MR images have been identified by an expert team of biologists and physicians. As a consequence of the deliberate decision to not idealize or simplify the segmentations the datasets contain very complex shapes with many small holes, disconnected islands and thin protrusions (Fig. 1). It is straight forward to use these datasets for applications they were originally designed for: finite difference based simulations of electromagnetic and thermal exposures. The datasets are, however, completely unsuitable for the FEA because of severe quality and consistency issues (e.g. blood vessels continuity and closure, connectivity of gray/white matter, etc.). Additionally, the goal of obtaining realistic segmented voxel data conflicts with the inherent need of FEA to use simplified, high-quality, manageable geometries. In this paper we present, evaluate and discuss the methods to generate high quality unstructured meshes directly from the large image datasets of the *Virtual Family* for large scale whole body simulations.

2. Related Work

For a general overview of the available literature related to meshing techniques see e.g. [2] and references therein. In essence, there are many reliable approaches for engineered objects, i.e., objects "well behaved", with regular and distinct features, often composed of primitives, as is often the case in mechanical design applications. Concerning medical applications, there are only very few algorithms present in the literature that would generate meshes directly from multi-label medical image data. The octree techniques [3, 4] generate meshes with consistent multi-material junctions, however the quality of the elements at the interfaces turns out to be very poor and needs further improvements. There are methods relying on Delaunay refinement [5, 6, 7]. In practice, however, even though the quality of the final mesh is good, the representation of the interfaces is not (jiggles). In addition, sometimes there are problems with the termination of this complex procedure for noisy or poorly resolved datasets. Some newer methods [8] improve the interface smoothness by protecting the interface points during the refinement process. They will, however, sometimes fail in practice due to under-resolved regions of high curvatures, as is unfortunately very often the case with MRI data.

3. Methods

3.1. Geometry Extraction

To obtain a good surface representation of given domains we proceed as follows:

- Convert the desired segmentation label field(s) into an implicit (*level set*) representation. Different choices are available for the embedding function, including signed distance or mollified step functions. It is important that the gradient of this function reasonably well approximates the surface normal.
- Smooth the resulting scalar field so as to remove stair-casing artifacts originating from the voxel representation.
- Compensate for smoothing induced volume loss by solving the *level set* equation $\frac{\partial \phi}{\partial t} + \vec{u} \nabla \phi = 0$ for the interface embedding function ϕ and the *interface advancing* velocity $\vec{u} = u_0 \nabla \phi$, with u_0 compensation parameter subject to the assumption that the gradient of the embedding function approximates the surface normal. By assuming that the embedding function is a signed distance transform, the above equations are greatly simplified, but they will require significant time to compute.
- Extract an explicit interface using a contouring algorithm like *marching cubes*.

The obtained surface mesh will be a good and smooth representation of the domain in question, but will be excessively sized and of very poor quality (many degenerate triangles). It needs therefore to be processed further, as presented below.

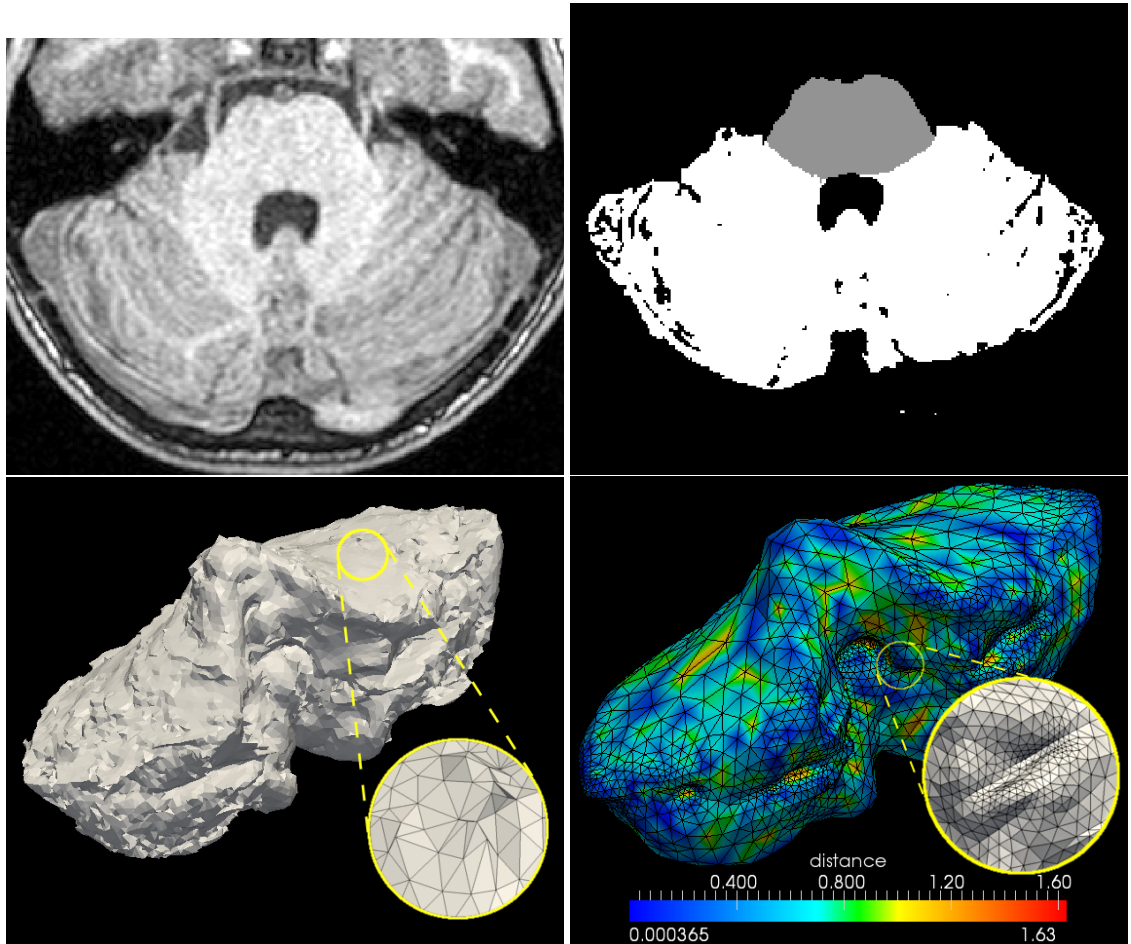


Figure 1: **Top left:** MRI scan of a human cerebellum. **Top right:** Tiny, narrow and disconnected features in the segmentation. **Bottom left:** Surface mesh obtained by naive contouring of the segmentation label field. Note badly conditioned surface elements (numerous degenerate ones are too thin to be visible). **Bottom right:** FEM-ready tetrahedron mesh colored with the distance (in mm) to the original voxel data. Note the mesh orthogonality.

3.2. Surface Remeshing

To generate a good uniform surface mesh we first decimate the original mesh using a variant of a topology preserving quadric decimation algorithm [9]. The resulting mesh is then iteratively smoothed and projected back onto its original in order to eliminate volume loss. The result is a very good uniform surface mesh, with global element size easily controlled by a requested reduction of the number of elements during decimation. It can be volume-meshed right away, but we further process it with a surface optimization method [10] to adapt the mesh density to the local curvature. It is fundamental that the mesh input to this procedure is already reasonably well conditioned, else precondition violations may result due to degenerated triangles, arbitrarily small angles, etc.

3.3. Volume Meshing

Any method capable of generating volumetric meshes from a fixed surface mesh can be used. There are many commercial as well as a few open source packages offering such functionality.

3.4. Compatible Interface Triangulations

The meshing techniques described so far enforce geometrical (typically with sub-voxel accuracy), but not topological compatibility of the triangulations between the neighboring domains (touching organs/tissues). Perhaps the simplest way to achieve the topological consistence is to map the bounding volume of the whole dataset with unstructured elements and simply transfer the label field from the original image data. This is ultimately robust in the computational geometry sense, delivers meshes of extremely high quality, provides compatible triangulations between domains, but obviously gives their worst geometric representation as the conformance to the domain boundaries is not enforced. Moreover, transfer of the labels from voxels to unstructured elements like tets is non-unique and can further contribute to interface jiggles. However, this may be still sufficient in very many situations. Unlike machines, living bodies do not always have precisely defined discontinuous interfaces between their components. Therefore, such representation may be sufficient in some cases when completed with a continuous smooth scalar field defining the material properties. To achieve better representation of the interface one can add various 3D Delaunay refinement methods [5, 6, 7, 8] to enforce the interface compliance.

A simple method offering better control of the geometrical fidelity of the interfaces is based on the idea of a *background material*. Arguably, in living bodies the organs often do not touch each other directly with a discontinuous interface. Instead, the regions in contact are often coated with fat, connective tissue or fluid. Under this assumption the mesh generation is straight forward. The largest domain is the background material, containing all the organs and always preventing their direct contact by a separating layer. Therefore it is sufficient to only mesh the background material with the method described before. All the contained organs will appear in this mesh as separated holes. These holes can be easily filled by any volume meshing procedure that will preserve the given (good) surface triangulation.

When the background material approach is not acceptable one can use a variant of *marching cubes* algorithm operating on discrete scalar fields. The interface in such a case is created exactly middle way between the adjacent voxels. This generates topologically compatible interfaces, unfortunately, retains the staircasing. We use a volume preserving windowed sinc function interpolation kernel to regularize the point coordinates [11] and achieve satisfactory results. The drawback is that the method requires clean and sufficiently resolved segmentations, else the interpolation kernel would generate exploding spikes at the noisy locations. To avoid this problem the segmentation has to be either manually corrected or smoothed automatically, as shown in Fig. 3.

When corrections to the segmentations are not possible, another method is to very slightly offset the embedding function (in the sub-voxel range) past the original segmentation border prior to the explicit surface extraction so as to generate geometrical intersections between the extracted domains. Using then boolean operations on these surfaces (a large number of different methods has been proposed in the computer graphics literature) one obtains a union grid of bad quality but geometrical and topological consistency between domains and a smooth representation of the interfaces. It can be now volume-meshed by e.g. re-meshing interface surfaces one at a time while recursively constraining the just added points in the triangulations of the following interfaces. Another option is to simply use a cut-cell octree based method as available in some commercial packages. A fundamental point is that the boolean operations on surface meshes are very sensitive to the condition of the input which must consist of well conditioned orientable manifolds or the boolean operations will fail due to numerical problems.

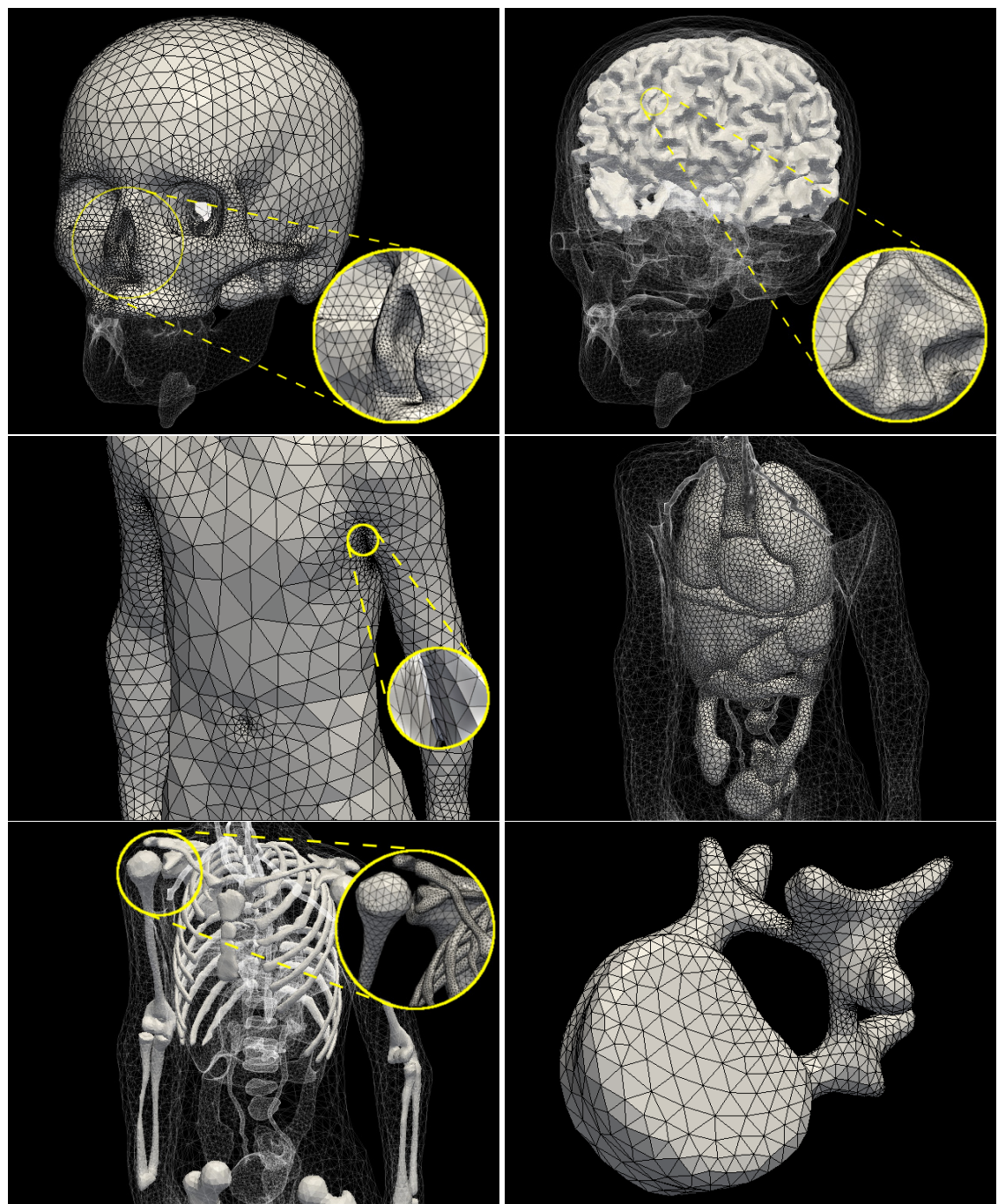


Figure 2: Examples of FEM models of a human body created from the *Virtual Family* datasets using the presented methods.

4. Results

We have applied the described methods to generate unstructured body fitted adaptive meshes from segmented medical image dataset of one *Virtual Family* member. While we are aware that correcting the input segmentations would fix many problems, we intentionally did not do so (neither manually nor automatically) to assess the methods' performance on "real life" non-perfect datasets. The first finding was that very thin structures like nerves or smaller vessels could not be meshed. They were often resolved with just 1-3 voxels in which cases the level set transform does not make any sense due to the obvious lack of continuity. However, we were easily able to process all medium to big sized tissues/organs (bigger than about 5 – 10mm), including the largest arteries and veins. The method proved very robust against disconnected tiny islands or noisy features by simply ignoring them in the smoothing step (the method is still volume preserving, i.e. no shrinkage results). Typical meshing times were about 15 minutes (including about 5 minutes of interactive choice of parameters) with notable exceptions of the skull and the white matter, where the total processing time reached a few hours (including trial and error interactivity of about 1h). Quality of all the meshes measured as the radii ratios ensured the absence of any flat elements (slivers). Apart from the quality, the meshes are also highly orthogonal, making them suitable also to simpler discretization schemes (e.g. cell face values are arithmetic means, cell face gradients can be easily computed, etc.), which would normally fail on non-orthogonal but otherwise good meshes. All the organs have geometrical, but not topological compatibility at the internal interfaces making them suitable to e.g. domain decomposition methods relying on cross domain interpolations. Some of the resulting meshes are presented in Fig. 1 and 2.

Next, we attempted to generate models with compatible triangulations at the interfaces for selected organ complexes. The method based on the Delaunay refinement was able to terminate even with the original segmentations. The result (Fig. 3, bottom right) is a huge mesh of several million high quality elements, with compatible, but somewhat jiggled internal interfaces. Most certainly, there will be applications where such a solution will be an acceptable option, e.g., by relying on additional smooth scalar field of tissue parameters derived from the original continuous gray level data.

We achieved very good results exploiting the *background material* approach. A potential drawback is that for very thin layers of the coating material very small elements have to be created, which can lead to excessive mesh sizes.

We were not able to obtain any satisfactory results with the method enforcing topological compatibility based on the discrete variant of the *marching cubes* without modifications of the segmentation data. The results obtained from this method inherently preserve staircasing artifacts and must be smoothed in some way. The interpolation kernel used in our volume preserving smoothing routine turned out to be too sensitive to the given noise, which resulted in many random spikes all over the surfaces. We found, however, that automatic smoothing of the segmentation based on the same level set idea as to extract the initial geometries (each label separately at a time) changed the situation dramatically. The meshes did not contain spikes anymore and their cross-domain triangulations were topologically compatible. The drawback is some loss of sharp features, even though the smoothing is volume preserving. Also, the approach "resolve or reject" may be unacceptable for some applications. But then again, while this approach is not an ultimate answer to the compatible triangulation problem, it will certainly be applicable in some situations.

We achieved very good results with the method relying on boolean operations on surface meshes. Here the segmentation corrections were not needed again, but manual corrections would probably give much better control over the more exact definition of interfaces. The surface meshes obtained by decimation and projected smoothing proved to be sufficiently well conditioned for a robust performance of the boolean surface operations (see Fig. 3, top right, bottom left). This resulted in very good, both geometrically and topologically compatible meshes with smooth interfaces.

All operations were performed on a 64-bit PC with the Intel 8-core Xeon processor, 32 GB RAM, linux operating system and the GNU compiler collection. Images were rendered using the Visualization Toolkit (VTK) from Kitware, Inc.

5. Conclusions

We have reviewed several techniques to generate unstructured meshes directly from the segmented medical image data. We have evaluated these methods on the *Virtual Family* datasets by generating over a hundred of unstructured models of various organs and tissues. Although none of the presented methods is an automatic solution that can be

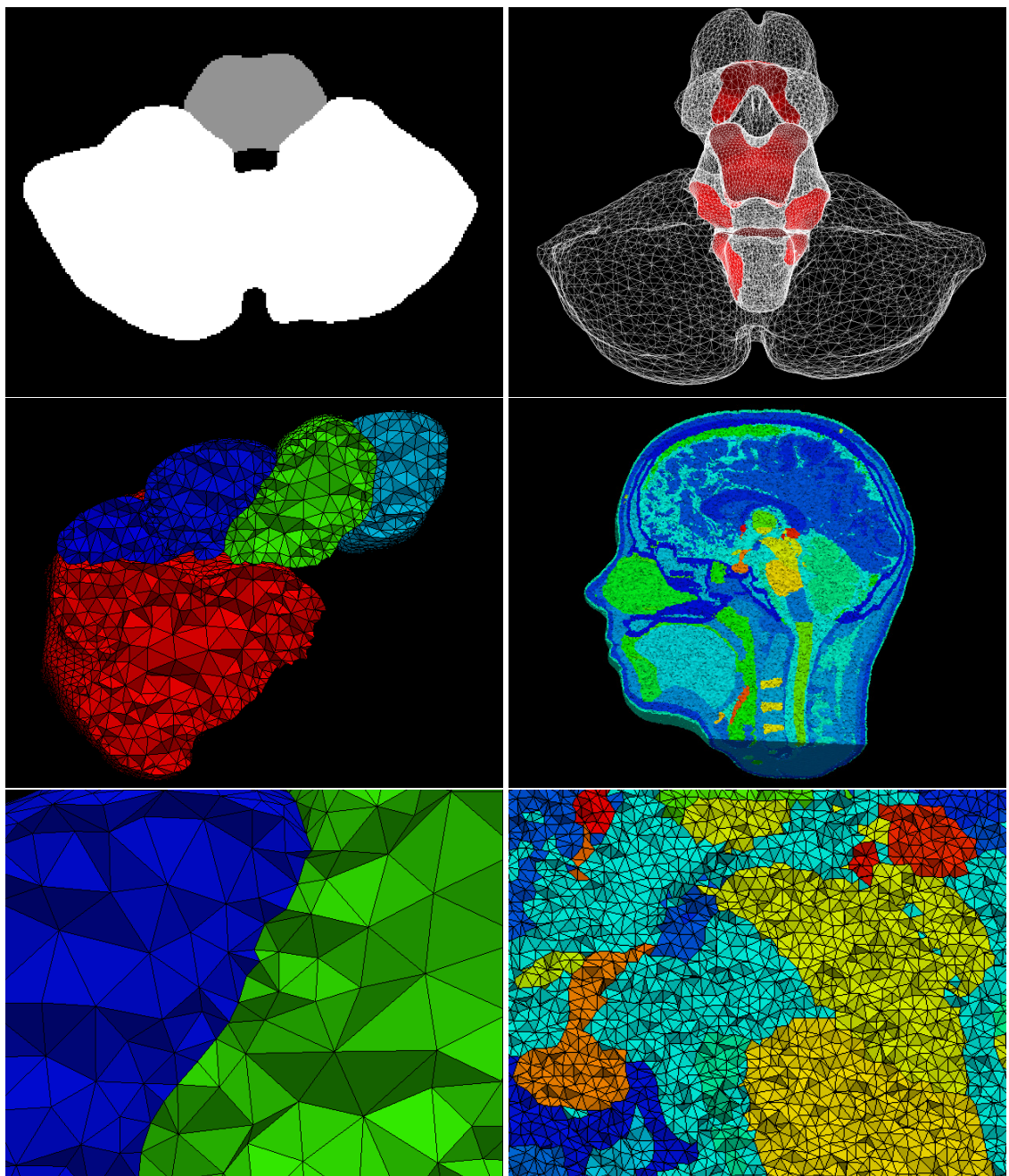


Figure 3: **Top left:** Automatically cleaned segmentation to facilitate compatible meshing discussed in the text (cf. Fig. 1). **Top right:** Common conforming compatible interfaces between brain sub-regions highlighted in red. **Middle:** Topologically compatible triangulations obtained with the boolean operations (left) and Delaunay refinement method (right) discussed in the text. **Bottom:** Magnified fragments of the images in the middle row.

applied to any input data in all possible cases, our evaluation aims to provide guidance in selecting the optimal method to generate a required anatomical model from segmented medical images.

If topologically compatible interfaces between the domains are not required, the presented procedures work quite reliably, almost automatically, and do not require a highly trained software engineer to operate them. Human supervision is generally only required to decide about the mesh size and refinement parameters. It is, however, rather sensitive to the (lack of) resolution and features must be resolved with sufficient accuracy or the meshes may contain erroneous elements in those one-voxel narrow passages, under-resolved high curvatures or three-voxels small sub-regions. Rejecting such tiny features (most conveniently in the segmentation) that are anyway on the edge of uncertainty has always resolved such problems.

To achieve topologically compatible interfaces while ensuring their high geometrical fidelity is not an easy task, both to implement and to operate. We found, however, that if the segmentation is of sufficient resolution and quality, and if the extracted geometrical surfaces are well conditioned, very good results can be achieved with optimal amount of user interaction.

References

- [1] A. Christ, W. Kainz, E. Hahn, K. Honegger, M. Zefferer, E. Neufeld, W. Rascher, R. Janka, W. Bautz, J. Chen, et al., The Virtual Family—Development of anatomical CAD models of two adults and two children for dosimetric simulations, *Physics in Medicine and Biology*.
- [2] D. Szczerba, R. McGregor, G. Székely, High quality surface mesh generation for multi-physics bio-medical simulations, in: LNCS, 2007, pp. 906–913.
URL http://dx.doi.org/10.1007/978-3-540-72584-8_119
- [3] M. A. Yerry, M. S. Shephard, Automatic three-dimensional mesh generation by the modified-octree technique, *International Journal for Numerical Methods in Engineering* 20 (11) (1984) 1965–1990.
URL <http://dx.doi.org/10.1002/nme.1620201103>
- [4] M. S. Shephard, M. K. Georges, Automatic three-dimensional mesh generation by the finite octree technique, *International Journal for Numerical Methods in Engineering* 32 (4) (1991) 709–749.
URL <http://dx.doi.org/10.1002/nme.1620320406>
- [5] L. Rineau, M. Yvinec, A generic software design for delaunay refinement meshing, *Computational Geometry* 38 (1-2) (2007) 100 – 110, special Issue on CGAL. doi:DOI: 10.1016/j.comgeo.2006.11.008.
URL <http://www.sciencedirect.com/science/article/B6TYS-4NDMN9J-2/2/123233326f16d98780ac47c7d3d49d32>
- [6] J. Pons, F. Ségonne, J. Boissonnat, L. Rineau, M. Yvinec, R. Keriven, High-quality consistent meshing of multi-label datasets (2007).
URL http://dx.doi.org/10.1007/978-3-540-73273-0_17
- [7] J.-D. Boissonnat, J.-P. Pons, M. Yvinec, From segmented images to good quality meshes using delaunay refinement (2009).
URL http://dx.doi.org/10.1007/978-3-642-00826-9_2
- [8] S.-W. Cheng, T. K. Dey, J. A. Levine, A practical delaunay meshing algorithm for a large class of domains (2008).
URL http://dx.doi.org/10.1007/978-3-540-75103-8_27
- [9] M. Garland, P. Heckbert, Surface simplification using quadric error metrics, in: Proceedings of the 24th annual conference on Computer graphics and interactive techniques, ACM Press/Addison-Wesley Publishing Co. New York, NY, USA, 1997, pp. 209–216.
- [10] J. Schöberl, Netgen an advancing front 2d/3d-mesh generator based on abstract rules, *Computing and Visualization in Science* V1 (1) (1997) 41–52.
URL <http://dx.doi.org/10.1007/s007910050004>
- [11] G. Taubin, T. Zhang, G. Golub, Optimal surface smoothing as filter design, *Lecture Notes in Computer Science* 1064 (1996) 283–292.